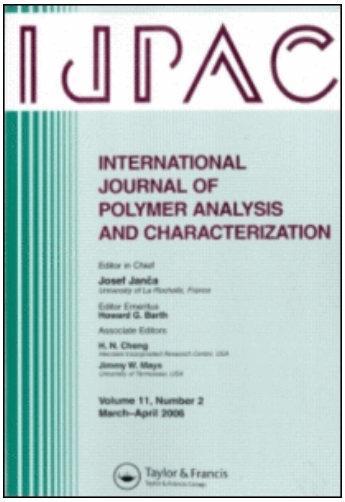

International Journal of Polymer Analysis and Characterization
Publication details, including instructions for authors and subscription information:
http://www.informaworld.com/smpp/title~content=t713646643

Organic-Inorganic Hybrid Materials 4: NMR Study of the Poly(imide-silica) Hybrids

T. C. Chang[a]; Y. T. Wang[a]; Y. S. Hong[a]; K. H. Wu[b]; T. R. Wu[c]
[a] Department of Applied Chemistry, Chung Cheng Institute of Technology, Tahsi, Taoyuan, Taiwan, Republic of China [b] The Army General Headquarters, Lungtan, Taoyuan, Taiwan, Republic of China [c] Chemical Systems Research Division, Chung Shan Institute of Science and Technology, Lungtan, Taoyuan, Taiwan, Republic of China

To cite this Article Chang, T. C. , Wang, Y. T. , Hong, Y. S. , Wu, K. H. and Wu, T. R.(2001) 'Organic-Inorganic Hybrid Materials 4: NMR Study of the Poly(imide-silica) Hybrids', International Journal of Polymer Analysis and Characterization, 6: 5, 403 — 413
To link to this Article: DOI: 10.1080/10236660108033957
URL: http://dx.doi.org/10.1080/10236660108033957

Int. J. Polym. Anal. Charact.,
2001 Vol. 6, pp. 403–413
Reprints available directly from the publisher
Photocopying permitted by license only

Organic–Inorganic Hybrid Materials 4: NMR Study of the Poly(imide–silica) Hybrids

T. C. CHANG[a,*], Y. T. WANG[a], Y. S. HONG[a], K. H. WU[b] and T. R. WU[c]

[a]*Department of Applied Chemistry, Chung Cheng Institute of Technology, Tahsi, Taoyuan, Taiwan 335, Republic of China;* [b]*The Army General Headquarters, Lungtan, Taoyuan, Taiwan 325, Republic of China;* [c]*Chemical Systems Research Division, Chung Shan Institute of Science and Technology, Lungtan, Taoyuan, Taiwan 325, Republic of China*

(Received 12 October 1999; In final form 25 October 1999)

The microstructure of the poly(imide–silica) hybrid materials containing various proportions of silica was examined by high-resolution solid-state ^{29}Si and ^{13}C nuclear magnetic resonance spectroscopy. The ^{29}Si—^{1}H cross-polarization (CP) process revealed that the Q^2, Q^3 and Q^4 species had different CP efficiency. Moreover, the time constant for the energy exchange between ^{1}H and ^{29}Si spin systems (T_{SiH}) for the siloxane units was less restricted by silica than by imide. The spin-lattice relaxation time in rotating frame ($T_{1\rho}^{H}$) of hybrids indicated that the ^{1}H spin diffusion between imide and siloxane units were on a nanometer scale.

Keywords: Poly(imide–silica); Hybrids; Nuclear magnetic resonance; Relaxation; Spin-diffusion

INTRODUCTION

Organic–inorganic hybrids are attractive materials with heat resistance, good mechanical and electrical properties, and radiation resistance.[1] The organic polymers combined with inorganic oxides using variations of the sol–gel method have become prevalent as a means of preparing organic–inorganic hybrid materials.[2] Employing

*Corresponding author.

the sol–gel reaction, the synthesis of the poly(imide–silica) hybrid (PI—SiO_2) has been reported.[3–16] Two main procedures have been used to prepare PI—SiO_2 hybrids. The first uses a mixture of a tetrafunctional silicon alkoxide and the PI without trialkoxysilyl functional group to produce composite materials.[3–9] The second creates bonding sites between the PI and the silica, resulting in homogeneous, hybrid materials.[10–16]

Several methods have been used to characterize the miscibility of organic–inorganic hybrids, including microscopy, scattering techniques, mechanical and thermal measurements, and spectroscopy. The relaxation processes can be influenced by several factors, such as the change of molecular mass, addition of a suitable polymer modifier, preparation of polymer hybrid, spinning under different conditions, and stretching. Different chemical and physical modifications for hybrids produce some changes of the molecular motions. NMR methods are sensitive to short range interactions. However, there are very few articles on the dynamics of PI—SiO_2 hybrids.[15] Thus a further study to estimate the extent of miscibility for these hybrids is carried out by NMR using relaxation time measurements. The technique of the rotating frame spin-lattice relaxation times ($T_{1\rho}$) is, owing to the low frequency and the restriction of spin- diffusion over the much shorter $T_{1\rho}$ times, more sensitive to the structural changes and molecular motions than those of the laboratory frame spin-lattice relaxation times (T_1).[17] However, the Si—H polarization transfer relaxation time constant (T_{SiH}) can be calculated from a double-exponential fit of the NMR line intensity *versus* contact time. To understand the scale of homogeneity of the hybrids, we have measured T_{SiH} and $T_{1\rho}^{H}$.

EXPERIMENTAL

Preparation of the PI—SiO_2 Hybrids

PI—SiO_2 hybrids prepared by sequential condensation reactions are shown in Scheme 1, and their theoretical schematic structures are shown in Figure 1.[15] Hybrids were designated so that, for example, 6A-30 denotes diamic acid reacted with about 30 wt% of tetramethoxysilane TMOS ($[H_2O]/[TMOS] = 6$). The nomenclature of D^i and Q^i

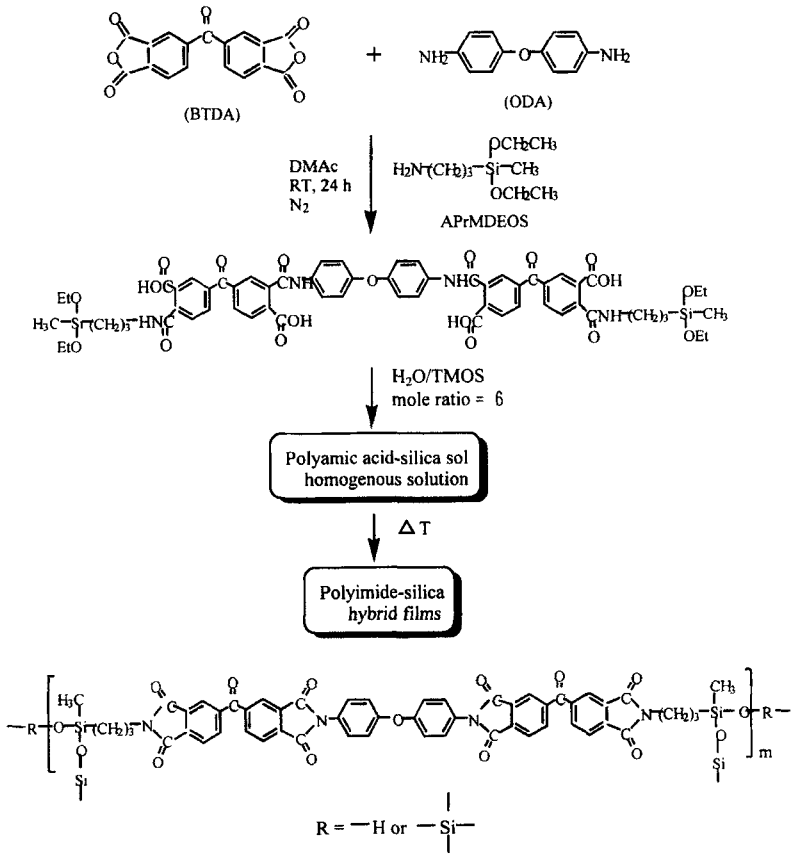

SCHEME 1

was taken from Glaser and Wilker[18], where i refers to the number of —O—Si groups bonded to the silicon atom of interest. D^i and Q^i denote species that have two organic side groups and no organic side group, respectively. Hybrid 6A without addition of TMOS was synthesized *via* a similar procedure for comparison. The hybrids 6A presented two siloxane bonds and one methyl group bonded to a silicon atom, giving a two-dimensional network material. However, the silanol group (Si—OH) that was formed during the hydrolysis of alkoxy groups in APrMDEOS and TMOS induced more cross-linked three-dimensional (D^i and Q^i) network materials for other hybrids.

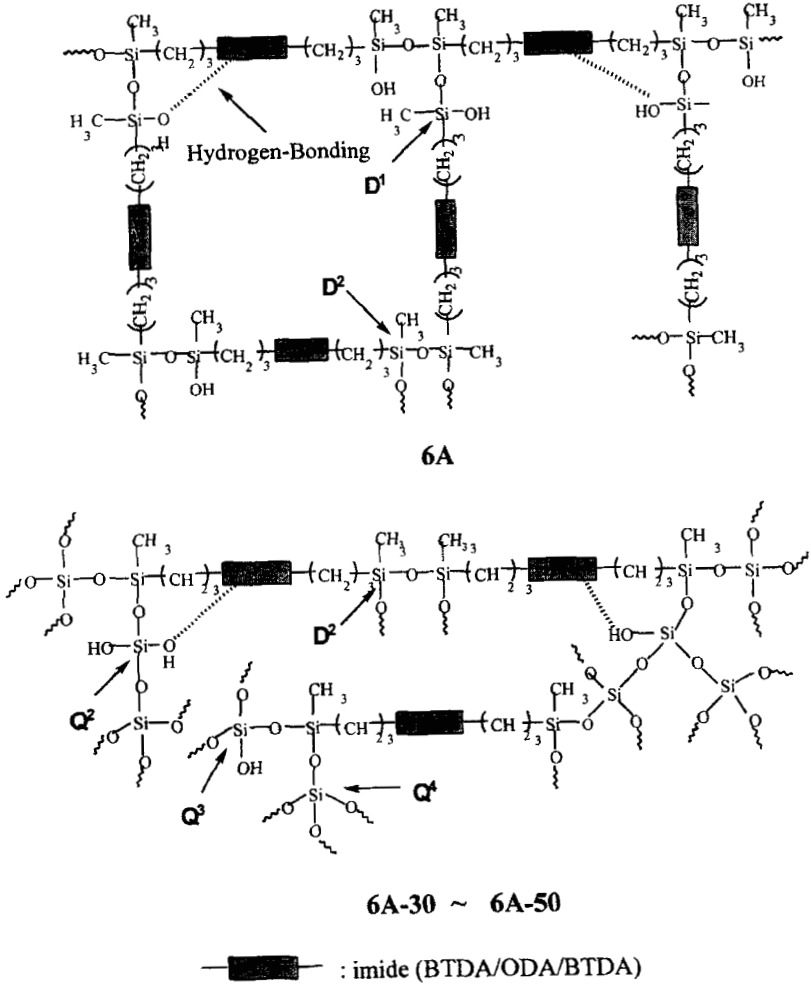

FIGURE 1 The theoretical structure of PI—SiO_2 hybrids.

Characterization of the PI—SiO_2 Hybrids

The structure of PI—SiO_2 hybrid was confirmed by its infrared (IR) spectrum (Bomem DA 3.002). For the sample prepared *via* the KBr pellets technique, the IR (KBr) bands are 1778 cm^{-1} (imide C=O symmetric stretching), 1718 cm^{-1} (imide C=O asymmetric stretching), 1382 cm^{-1} (C—N stretching), 1080 cm^{-1} (Si—O—Si vibration), and

720 cm^{-1} (imide ring deformation). The ^{13}C and ^{29}Si nuclear magnetic resonance (NMR) spectra of the solid-state PI—SiO_2 hybrids were determined (Bruker MSL-400) by using the cross-polarization/magic angle spinning (CP/MAS) technique. ^{29}Si NMR spectrum of 6A hybrid had two peaks at −9.6 and −20.4 ppm, corresponding to D^1 and D^2 structures, respectively. ^{29}Si NMR spectra of hybrids 6A-30, 6A-50 and 6A-70 showed four peaks about at −16.8, −91.4, −100.4 and −108 ppm corresponding to D^2, Q^2, Q^3, and Q^4, respectively. ^{13}C CP/MAS NMR spectra of the PI—SiO_2 hybrids were nearly identical. A set of peaks for imide dimer was observed at around 193, 167, 159 and 140–124 ppm arising from the benzophenone carbonyl, imide carbonyl, aryl carbons with oxygen substituents, and various aromatic carbons, respectively. The other set of peaks was observed at around 41, 22, 14 and −0.06 ppm that correspond to —NCH_2—, —CH_2—, —CH_2Si— and —$SiCH_3$, respectively.

CP contact time studies can produce Si—H polarization transfer constant (T_{SiH}). The ^1H—^{29}Si spin contact time in the rotating frame with the Hartmann–Hahn condition was typically about 5 ms, but optimized in the range between 0.5 and 20 ms. Proton spin-lattice relaxation times in the rotating frame ($T_{1\rho}^H$) were measured by using a ^1H spin-lock τ-pulse sequence followed by cross-polarization. The ^1H 90° pulse width was 4.5 μs, and the CP contact time was 2 ms. The length of delay time τ ranged from 0.1 to 25 ms for $T_{1\rho}^H$.

RESULTS AND DISCUSSION

Cross Polarization Process

In the conventional CP process under Hartmann–Hahn conditions, ^1H and ^{29}Si spin systems are spin-locked in the rotating frames and thermally in contact with each other, thus exchanging their energies. The respective spin systems also exchange energies with the surrounding thermal reservoir, the so-called lattice. Figure 2 gives an example of the effect of contact time t on the ^{29}Si resonance of the 6A-50 hybrid. Intensities in the Figure 2 reflect local cross-polarization dynamics which may vary from site to site. According to the simple theory in this CP process, magnetization $M_c(t)$ is expressed as a

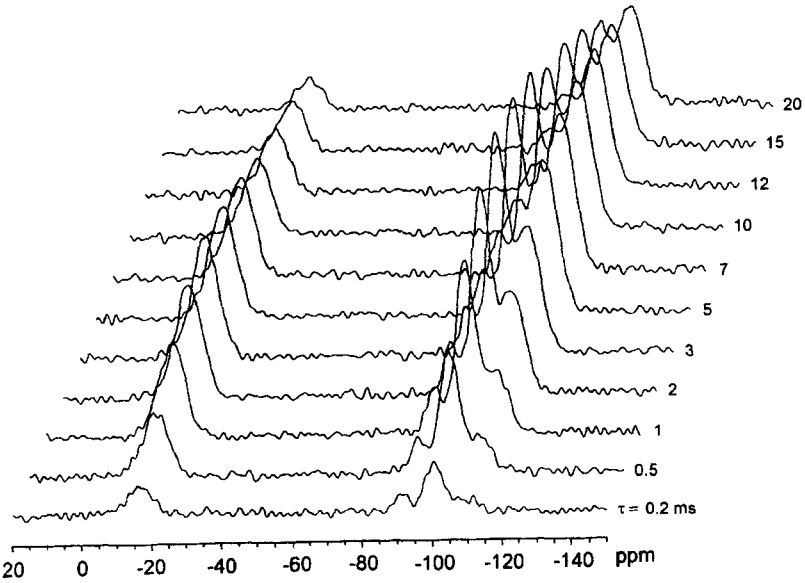

FIGURE 2 Stacked plot of the CP-MAS spectra of 6A-50 hybrid as a function of contact time.

function of the contact time as follows:[19]

$$M_c(t) = M_e\left[\exp(-t/T_{1\rho}^{H}) - \exp(-t/T_{SiH})\right]$$

Here, M_e, is the ^{29}Si equilibrium magnetization obtained when both spin systems fully interact with each other without any energy exchange with the lattice and therefore this value is proportional to the concentration of a given ^{29}Si nucleus in a material. T_{SiH} is the time constant for the energy exchange between ^{1}H and ^{29}Si spin systems, and $T_{1\rho}^{H}$ is the spin-lattice relaxation time in a rotating frame. This equation indicates that the ^{29}Si magnetization appears at the rate of the order of $(T_{SiH})^{-1}$ and disappears at the rate of $(T_{1\rho}^{H})^{-1}$.

Figure 3 shows a semilogarithmic plot of the peak intensity as a function of the contact time for the silicon in the 6A-50 hybrid. A steeper slope is an indication of faster transfer of magnetization (shorter T_{SiH}) or faster relaxation by spin diffusion (shorter $T_{1\rho}^{H}$). The values of T_{SiH} and $T_{1\rho}^{H}$ estimated by curve-fitting are summarized in

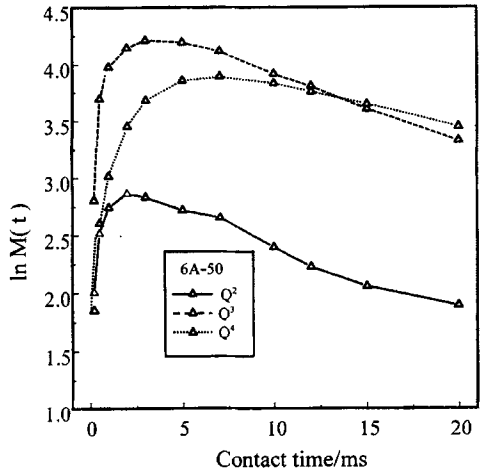

FIGURE 3 Semilogarithmic plot of the peak intensity of the Q^3, Q^3 and Q^4 species shown in Figure 2 as a function of contact time.

TABLE I T_{SiH} and $T_{1\rho}^H$ values of the respective resonance lines of PI—SiO_2 hybrids

		$T_{SiH}(ms)$				$T_{1\rho}^H(ms)$			
	δ/ppm ^{29}Si	6A	6A-30	6A-50	6A-70	6A	6A-30	6A-50	6A-70
D^2	−20.3	0.9	0.9	0.8	1.0	18.2	18.6	14.0	27.0
Q^2	−91.5	–	2.0	1.2	1.2	–	21.0	17.0	14.4
Q^3	−100.0	–	0.4	0.3	0.5	–	28.3	16.9	25.3
Q^4	−107.0	–	1.7	1.7	1.8	–	44.8	26.1	63.7

Table I. The Q^2 structure displays longer T_{SiH} relaxation than the Q^3 structure, although it has the largest number of relatively close protons. The result may be due to greater motion for the Q^2 structure. However, T_{SiH} and $T_{1\rho}^H$ values for Q^3 species are smaller than that for Q^4 species as shown in Table I. It indicates that the Q^3 centers contains protons that can provide the Si—H dipolar coupling. The low CP efficiency of the Q^4 species may be due to a few nearby protons in the material matrix to facilitate the transfer of polarization. Moreover, the curve in Figure 4 is linear that suggests that large-scale phase separation of Q^4 species does not occur in these materials. The ^{29}Si atoms of Q^4 species must be within approximately 10 Å of a proton to facilitate polarization transfer.[19]

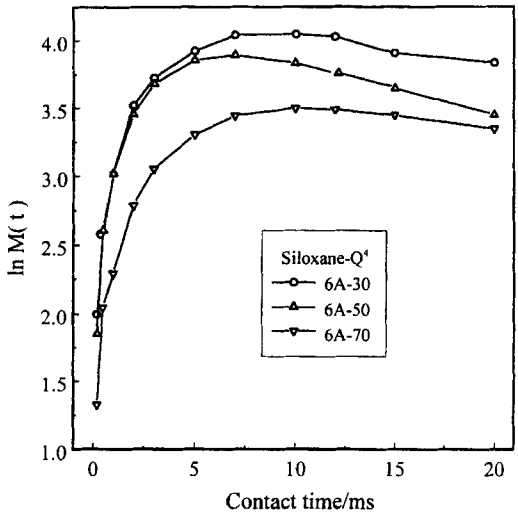

FIGURE 4 Semilogarithmic plot of the peak intensity of the Q^4 species as a function of contact time.

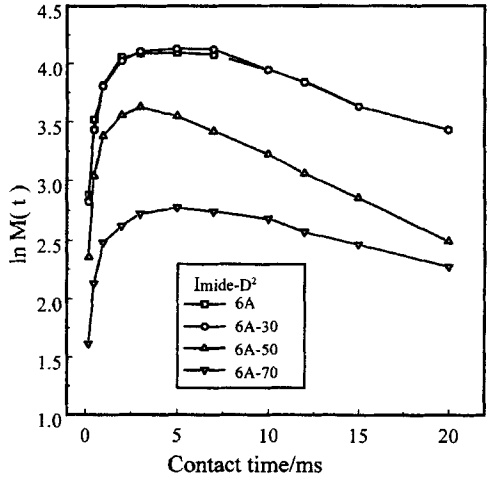

FIGURE 5 Semilogarithmic plot of the peak intensity of the D^2 species as a function of contact time.

Figure 5 shows a semilogarithmic plot of the peak intensity *versus* the contact time for the D^2 silicon of hybrids. It indicates that the intensities of the D^2 resonance in PI—SiO_2 hybrids reach a maximum

approximately at 2.5 ms that is less dependent on the silica content. The values of $T_{SiH}(D^2)$ and $T_{1\rho}^{H}(D^2)$ estimated by the curve-fittings are listed in Table I. The results reveal that the flexibility of the free siloxane chains is less restricted by silica than by imide.

^{1}H Spin-lattice Relaxation Time in the Rotating Frame

The relaxation time $T_{1\rho}^{H}$ of the protons is a quantity which is averaged within a domain of 1–2 nm diameter. $T_{1\rho}^{H}$ can therefore be treated as a phase quantity, at least in those cases where there is sufficient dipolar coupling among the protons to provide spin-diffusion over the range of 1–2 nm. It should be noted that the $T_{1\rho}^{H}$ values in Table I are obtained by the analysis of the CP process. Based on the spin-locking mode employed in $T_{1\rho}^{H}$ measurement, the magnetization of resonance is expected to decay according to the following exponential function: [19]

$$M_\tau = M_0 \exp[-\tau/T_{1\rho}^{H}].$$

Here, τ is delay time used in the experiment and M_τ corresponds to resonance intensity. Table II lists the $T_{1\rho}^{H}$ values of the respective carbon of hybrids measured by using the standard pulse sequence. The cause of the difference is not clear at present but the values indirectly determined may contain some unknown contributions in the CP process. It seems, therefore, plausible to discuss relative changes in $T_{1\rho}^{H}$ instead of absolute values, as in previous section. As is clearly in Table II, the $T_{1\rho}^{H}$ values for imide units are in agreement with those for siloxane units. This finding reveals that the ^{1}H spin diffusion between imide and siloxane units is very fast although their molecular mobility

TABLE II $T_{1\rho}^{H}$ and L values of the respective resonance lines of PI—SiO_2 hybrids

	$T_{1\rho}^{H}(ms)/T_2(\mu s)/L(nm)$			
δ/pmm ^{13}C	6*A*	6*A*-30	6*A*-50	6*A*-70
166.7	11.2	12.4	10.5	13.8
134.8	12.5/27.3/2.0	12.4/27.5/2.1	8.4/25.6/1.6	13.8/25.6/1.3
14.0	18.0	14.9	12.2	14.3
1.0	17.0/30.7/2.4	14.3/33.7/2.1	11.3/40.8/1.8	14.1/43.9/1.8

are different. It is, therefore, concluded that most of imide and siloxane units are compatible in hybrids in a scale of several nanometers.

A fast spin-diffusion occurs among all protons in hybrids, which averages out the whole relaxation process. Thus, the domain size of hybrids is smaller than the spin-diffusion path length within $T_{1\rho}^{H}$ time. The spin-diffusion path length, L, can be estimated using the following equation: [20]

$$\langle L^2 \rangle = (T_{1\rho}^{H}/T_2)\langle l_0^2 \rangle$$

Here l_0 is the distance between protons and has a typical value on the order of 0.1 nm. T_2 is the proton spin–spin relaxation time, and $\langle L^2 \rangle$ is the mean-square distance over which magnetization is transported. The values of T_2 is obtained in a previous paper [15] and then $\langle L^2 \rangle$ can be evaluated (Tab. II). It can be seen that the L values of the hybrids are clearly around 2 nm.

CONCLUSIONS

The microstructures of the poly(imide–silica) hybrid materials, prepared *via* condensation, imidization, and sol–gel techniques by mixing TMOS with a imide precursor, were characterized by high resolution solid-state NMR spectroscopy. The CP efficiencies of the Q^3 and Q^4 species were determined by local chemical environment of the protons which provided Si—H dipolar coupling. A more complex CP dynamics were observed for the Q^4 species as these can be accounted for by considering the lower hydrogen concentration in the vicinity of Si. The greater motion of the Q^2 structure resulted in longer T_{SiH} relaxation times than the Q^3 structure. Moreover, the values of $T_{SiH}(D^2)$ and $T_{1\rho}^{H}(D^2)$ were less dependent on the silica content because the flexibility of the free siloxane chains was less restricted by silica than by imide. The ^1H spin-diffusion between imide and siloxane units was very fast although their molecular mobilities were different. From spin-diffusion path length examinations, the distance between the imide and the siloxane units in the hybrids are roughly on a nanometer scale.

Acknowledgments

The authors thank the National Science Council of the Republic of China (Grant NSC 88-2113-M014-004). We would also like to thank Miss S. Y. Fang for her expert technical assistance.

References

[1] J. E. Mark, C. Y. C. Lee and P. A. Bianconic, Hybrid Organic–Inorganic Composites, *ACS Symposium Series 585*, American Chemical Society: Washington, DC, 1995.
[2] A. Morikawa, Y. Iyoku, M. Kakimoto and Y. Imai (1992). *J. Mater. Chem.*, **2**, 679.
[3] E. Theberge (1981). *Polym. Plast. Technol. Eng.*, **16**, 41.
[4] M. Nandi, J. A. Conklin, J. L. Salviati and A. Sen (1990). *Chem. Mater.*, **2**, 772.
[5] E. Breval, M. L. Mulvihill, J. P. Dougherty and R. E. Newnham (1992). *J. Mater. Sci.*, **27**, 2397.
[6] A. Morikawa, Y. Iyoku, M. Kakimoto and Y. Imai (1992). *Polym. J.*, **24**, 107.
[7] A. Morikawa, H. Yamaguchi, M. Kakimoto and Y. Imai (1994). *Chem. Mater.*, **6**, 913.
[8] K. Gaw, H. Suzuki, M. Kakimoto and Y. Imai (1996). *Mater. Res. Soc. Symp. Proc.*, **6**, 435.
[9] S. Goizet, J. C. Schrotter, M. Smaihi and A. Deratani (1997). *New J. Chem.*, **21**, 461.
[10] L. Mascia and A. Kioul (1994). *J. Mater. Sci. Lett.*, **13**, 641.
[11] S. Wang, Z. Ahmad and J. E. Mark (1994). *Macromol. Rep.*, **A31**, 411.
[12] L. Mascia and A. Kioul (1995). *Polymer*, **36**, 3649.
[13] L. L. Beecroft, N. A. Johnen and C. K. Ober (1997). *Polym. Adv. Tech.*, **8**, 289.
[14] P. Sysel, R. Pulec and M. Maryska (1997). *Polym. J.*, **29**, 607.
[15] K. H. Wu, T. C. Chang, Y. T. Wang and Y. S. Chiu (1999). *J. Polym. Sci. Polym. Chem.*, **37**, 2275.
[16] Y. Y. Chen and J. O. Iron (1999). *Chem. Mater.*, **11**, 1218.
[17] R. A. Komoroski Ed., *High Resolution NMR Spectroscopy of Synthetic Polymers in Bulk*, VCH Publishers, Florida, 1986.
[18] R. H. Glaser and G. L. Wilkes (1988). *Polym. Bull.*, **19**, 51.
[19] M. Mehring, *Principles of High Resolution NMR in Solids*, 2nd edn., Springer, Berlin, 1983.
[20] V. J. McBriety and D. C. Douglass (1981). *Macromol. Rev.*, **16**, 295.